

## Estimating platform kinematics using multi-antenna GNSS



Andreas Wieser and Roland Aschauer

### Abstract

The position, velocity, and attitude of a moving platform can be determined in realtime using GNSS with three or more antennas rigidly mounted on the platform. Objects shading satellite signals and causing multipath effects are a major concern for practical applications. In this contribution we derive the observation equations relating the platform parameters directly to the undifferenced pseudo-range, carrier-phase, and Doppler observations. We demonstrate that this approach is superior to deriving the platform kinematics from the kinematics of the individual GNSS antennas because it yields higher redundancy and offers a useful option for mitigating multipath effects created by the platform itself.

**Keywords:** GNSS, platform, attitude, positioning, multipath

### Kurzfassung

Position, Geschwindigkeit und Orientierung einer bewegten Plattform können mit Hilfe von drei oder mehr auf der Plattform fix montierten GNSS Antennen in Echtzeit bestimmt werden. Eine Herausforderung stellen dabei Plattform-Aufbauten dar, welche die Satellitensignale abschatten und Mehrwegeeffekte verursachen. Wir leiten in diesem Beitrag die Beobachtungsgleichungen her, welche die gesuchten Plattform-Parameter direkt mit den undifferenzierten Pseudostrecken-, Trägerphasen- und Dopplerbeobachtungen verknüpfen. Die Schätzung unter Verwendung dieser Beobachtungsgleichungen ist der Bestimmung der Plattform-Kinematik aus den Trajektorien der einzelnen GNSS Antennen überlegen, weil die Redundanz höher ist und sich eine praktische Möglichkeit zur Reduktion der negativen Auswirkungen von Mehrwegeeffekten und Abschattungen durch die Plattform selbst ergibt.

**Schlüsselwörter:** GNSS, Plattform, Lage, Positionierung, Mehrwegeeffekte

### 1. Introduction

Applications like mobile mapping, guidance and control of construction machines, hydrographic surveying or guidance of a slip form require the position and spatial orientation of a moving platform to be estimated accurately and reliably. The Institute of Geodesy and Geophysics at the Vienna University of Technology has established a research focus on platform navigation with particular interest in kinematic positioning and attitude determination at the centimeter and sub-degree level. Experimental investigations are carried out using a mobile robot which the Institute acquired lately (Fig. 1).

While GPS has initially been established for positioning, navigation and timing, it was an obvious idea to derive also the attitude i.e., spatial orientation, of a platform from GPS once relative positions of nearby antennas could be estimated with mm to cm accuracy, see e.g. [6]. In a PhD thesis carried out at the Stanford University, Clark Cohen developed a multiplexing receiver for attitude determination and related the attitude to the single-difference carrier-phase observations collected by a single receiver connected to several

GPS antennas [2]. This allowed estimating platform attitude directly from the GPS observations rather than computing it through a Helmert transformation. This approach also avoided the problem of handling the time offset between multiple non-synchronized receivers. Subsequently, optimum configurations of multi-antenna arrays for attitude determination were studied and found to be 4 antennas arranged in a tetrahedron [10]. By taking the time derivatives of the attitude equations given in [2], Ueno et al. [11] developed



Fig. 1: Autonomous robot equipped with multi-sensor system for kinematic positioning and mobile mapping

equations for estimating attitude rate directly from single-differenced Doppler observations.

Less attention has been paid to the simultaneous estimation of highly accurate position, velocity and attitude (PVA), and its potential benefit for effective mitigation of platform multipath and obstruction effects. However, these are of major importance for applications like the ones mentioned above and are the motivation for this contribution. A major challenge when using multi-antenna GNSS for platform PVA determination in applications to construction and surveying engineering is the selection of suitable antenna locations on the platform (machine). These locations cannot be freely chosen such as to provide optimum GNSS signal reception and data quality. Usually, they are restricted to parts of the platform where the antennas can be rigidly mounted but do not mechanically interfere with normal operation of the machine.

The antennas will therefore typically be subject to obstruction of satellite signals by parts of the platform. This affects the redundancy and the geometry negatively and thus impairs precision and reliability. However, these parts of the platform will typically also act as signal reflectors, see Fig. 2, and thus cause multipath effects which may be as large as about 5 cm at the individual carrier-phase observation level. The effect on the estimated coordinates may be of similar magnitude. This impairs the accuracy of the results and may be a significant challenge for quality control in the context of reliability and of outlier detection. The effect is even worse if the reflector is cylindrically or spherically shaped (see Fig. 2b). All satellite signals which are not obstructed may then be subject to (strong) multipath effects.

Furthermore, reflecting objects on the platform are usually close to the receiving antenna. The multipath error consequently oscillates with a period of several minutes up to half an hour or even more unless the platform exhibits significant attitude changes at shorter time scales. This can be derived from the well-known equations describing multipath error oscillations, see e.g. [4]. So, the multipath effects are virtually stationary and cannot be mitigated significantly by averaging over a few epochs or by filtering. Thus they are a significant challenge for machine guidance, platform navigation and similar applications.

A potential solution is the use of specially designed antennas with high attenuation close to the antenna horizon, see [1]. However, this will not be successful for near-boresight reflected signals

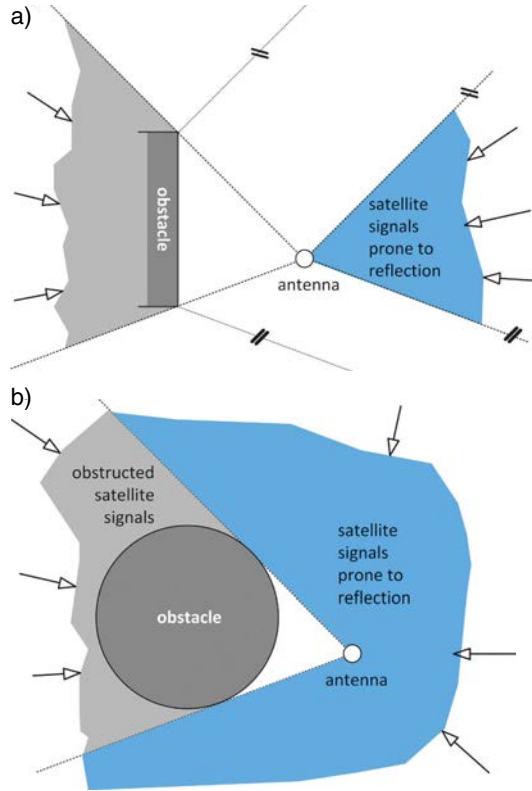


Fig. 2: Signal obstruction and reflection caused by a planar obstacle (a) and by a spherical obstacle (b) in the vicinity of a GNSS antenna; satellite (sender) assumed at infinite distance in direction of shaded areas.

(e.g. with high elevation satellites) and it will introduce an unwanted reduction of signal strength and availability of clear signals. We consider the use of suitably tuned microwave absorbing material (e.g. foam) a more suitable means for preventing reflections at the platform from reaching the GNSS antennas, see Fig. 3. If the absorbing screens are properly shaped and mounted, they will not introduce additional signal obstruction and thus not deteriorate the satellite availability further. However, they will avoid near-field multipath effects of the satellite signals actually received. The drawback is that the position and velocity of the individual antennas may not be observable from the GNSS observations anymore because of the signal obstruction. On the other hand, it is not necessary to estimate the individual antenna positions for the applications mentioned above. Instead, three or more antennas rigidly connected to the same platform can be used to collect raw data for estimating the position and velocity of the arbitrarily chosen platform origin. Band the plat-

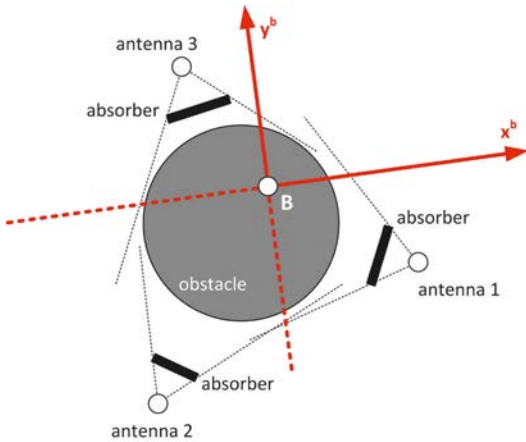


Fig. 3: Multi-antenna arrangement with microwave absorbing screens (absorbers) and platform coordinate frame (b-frame)

form attitude i.e., the orientation of the platform coordinate axes with respect to an earth fixed frame instead. Due to the lever arm of the individual antennas it is necessary to include the attitude rate as a nuisance parameter if the platform velocity is estimated.

In the following we will derive the observation equations linking the platform PVA to the undifferenced GNSS observations taking into account that there is no difference between GPS and any other GNSS as far as these equations and their practical applicability are concerned. We assume that raw GNSS observations from a nearby reference station are available and that double differenced (DD) pseudorange and carrier phase observations involving this reference station are used along with undifferenced Doppler observations obtained at the platform. (There is no practical benefit from using Doppler observations obtained at the stationary reference site or from processing DD Doppler observations.) In comparison with the previously published approaches based on single difference measurements obtained at the platform, this approach allows fully exploiting any potential redundancy, in particular when processing a maximum set of linearly independent DD observations rather than DD observations obtained using a reference-station/rover-station scheme. A useful algorithm for finding such a maximum set of DD can be found in [8].

When deciding whether individual terms need to be taken into account or may be neglected, we will consider terms negligible if they affect the carrier-phase and Doppler observation by less than 0.5 mm and 0.5 mm/s, respectively.

In correspondence with the applications mentioned above we will assume that the platform moves with a speed of less than 10 m/s, rotates with a rate of less than 0.6 rad/s (180° within 5 s) and that the lever arms are less than 10 m in length. Nevertheless, we will also indicate how the results relate to larger platforms or faster moving ones and are thus applicable to other applications than the ones mentioned above.

**2. Coordinate systems and transformations**

The locations of the GNSS antennas with respect to the platform, i.e., their coordinates expressed in the right-handed Cartesian “body-frame” (b-frame), are assumed to be known. The transformation of these coordinates to the earth-centered-earth-fixed frame (e-frame), e.g. ITRF2005, can be expressed as follows:

$$\mathbf{X}_i^e = \mathbf{X}_B^e + \mathbf{C}_b^e \mathbf{X}_i^b \tag{2.1}$$

with

$\mathbf{X}_i^e, \mathbf{X}_i^b$  ... coordinates of antenna  $i$  expressed in e- and b-frame, respectively,

$\mathbf{X}_B^e$  ... coordinates of origin of b-frame expressed in e-frame, and

$\mathbf{C}_b^e$  ... b-frame to e-frame rotation matrix.

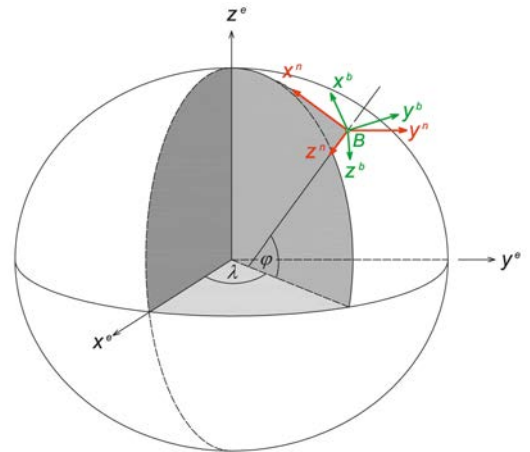


Fig. 4: Earth-centered-earth-fixed frame (e), navigation frame (n), and body (b) frame

For convenience, the b-frame to e-frame rotation matrix is split into a rotation with respect to the local level frame (n-frame) and a rotation of the local level frame with respect to the e-frame, see e.g. [5, §1.5 and § 5]:

$$\mathbf{C}_b^e = \mathbf{C}_n^e \mathbf{C}_b^n \quad (2.2)$$

with

$$\mathbf{C}_n^e = \begin{bmatrix} -\sin \varphi_B \cos \lambda_B & -\sin \lambda_B & -\cos \varphi_B \cos \lambda_B \\ -\sin \varphi_B \sin \lambda_B & \cos \lambda_B & -\cos \varphi_B \sin \lambda_B \\ \cos \varphi_B & 0 & -\sin \varphi_B \end{bmatrix} \quad (2.3)$$

where  $\varphi_B$  and  $\lambda_B$  indicate the ellipsoidal coordinates of the b-frame origin, and the axes of the n-frame point towards North, East and Down, as visualized in Fig. 4. The attitude of the platform can be described conveniently using yaw ( $\alpha$ ), pitch ( $\chi$ ) and roll ( $\eta$ ) which represent angles of sequential rotation according to

$$\mathbf{C}_b^n = \mathbf{R}_3(-\alpha) \mathbf{R}_2(-\chi) \mathbf{R}_1(-\eta), \quad (2.4)$$

where  $\mathbf{R}_k(\theta)$  is a rotation matrix describing the counter-clockwise rotation of a right-handed coordinate system about its  $k$ -th axis, see Fig. 5. If the platform is only slightly tilted, the yaw angle equals approximately the geodetic azimuth of the  $x^b$ -axis.

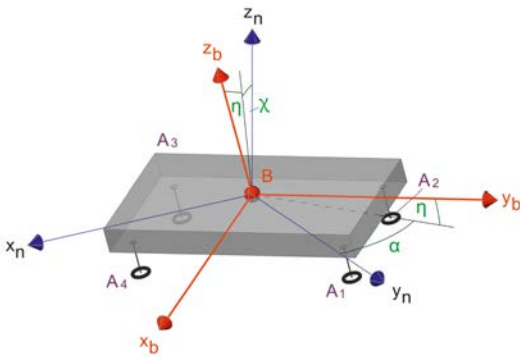


Fig. 5: Relative orientation of platform with respect to n-frame, expressed using pitch ( $\chi$ ), roll ( $\eta$ ) and yaw ( $\alpha$ ) angles ( $z^n$ -axis in reality pointing downwards; view is upside down for graphical reasons).

### 3. Position and attitude

The one-way carrier phase measurement between the receiving antenna  $i$  and the satellite  $j$ , can be expressed in units of meters as

$$\phi_i^j = \lambda \cdot \Phi_i^j = \rho_i^j - \lambda \cdot N_i^j + \dots \quad (3.1)$$

with

$$\rho_i^j = \|\mathbf{X}_j^e - \mathbf{X}_i^e\| = \sqrt{(\Delta \mathbf{X}_{ij}^e)^T \cdot \Delta \mathbf{X}_{ij}^e} \quad (3.2)$$

and

$\Phi_i^j$  ... carrier phase observation (in cycles)

$\lambda$  ... wavelength (in m/cycle)

$N_i^j$  ... one-way carrier phase integer ambiguity (in cycles)

In this equation, almost all terms which are treated identically with platform positioning as with individual point positioning or which are irrelevant for the present discussion, have been omitted for clarity. Without further discussion it is assumed that the Sagnac correction is properly applied to the satellite position such that eq. (3.2) actually represents the geometric distance between the satellite and the receiver expressed in the e-frame. A comprehensive discussion of the entire observation equation can be found in [7], [9] or other standard textbooks on GPS.

The non-linear measurement equations (3.1) are linearized at a suitable approximation in order to estimate the unknown parameters using linear estimators based on a chosen optimization criterion like maximum likelihood or minimum mean square error. This linearization yields the linearized observation equations

$$\underbrace{\phi_i^j - (\phi_i^j)_o}_{=: y_{\phi_i^j}} = \underbrace{\frac{\partial \phi_i^j}{\partial (\mathbf{X}_i^e)^T} \cdot d\mathbf{X}_i^e}_{\dots + \varepsilon_i^j + O^2} + \underbrace{\frac{\partial \phi_i^j}{\partial N_i^j} \cdot dN_i^j}_{=: e_{\phi_i^j}} + \dots \quad (3.3)$$

with the carrier phase measurement  $(\phi_i^j)_o$  computed from the assumed or predicted values of all parameters, and the original error term lumped together with the neglected higher order terms  $O^2$  into the residual  $e$ . From eq. (3.2) one can easily derive that the partial derivative with respect to the coordinates of the receiving antenna is the negative receiver to satellite unit vector expressed in the e-frame i.e.,

$$\frac{\partial \phi_i^j}{\partial (\mathbf{X}_i^e)^T} = -(\mathbf{a}_{ij}^e)^T. \quad (3.4)$$

The derivative with respect to the integer ambiguity is just the negative wavelength but does not need to be discussed any further here, because ambiguity resolution in the model derived here is carried out using the usual strategies and is thus not within the scope of the paper. However, as stated above, we aim at estimating the coordinates of the platform origin rather than those of the individual antennas. So, instead of the usual derivative with respect to  $\mathbf{X}_i^e$  we need the one with respect to  $\mathbf{X}_B^e$ . We can easily obtain it tak-

ing into account eq. (2.1) and applying the chain rule:

$$\frac{\partial \phi_i^j}{\partial (\mathbf{X}_B^e)^T} = \frac{\partial \phi_i^j}{\partial (\mathbf{X}_i^e)^T} \cdot \frac{\partial \mathbf{X}_i^e}{\partial (\mathbf{X}_B^e)^T}. \quad (3.5)$$

The first term on the right hand side is the usual derivative w.r.t. antenna position as given in eq. (3.4). The second term on the right hand side is a  $3 \times 3$  matrix which can be computed from eq. (2.1), e.g. by calculating each of the nine elements of the matrix separately. The result can be written in compact form using the Kronecker-product  $\mathbf{A} \otimes \mathbf{B} = [a_{ij} \mathbf{B}]$  which creates copies of the second matrix scaled by the elements of the first, and the  $\text{vec}$  operator which creates a column vector by stacking the columns of a matrix starting with the leftmost one:

$$\frac{\partial \mathbf{X}_i^e}{\partial (\mathbf{X}_B^e)^T} = \mathbf{I} + \left[ \mathbf{I}_3 \otimes (\mathbf{C}_b^n \mathbf{X}_i^b)^T \right] \cdot \frac{\partial \text{vec} \mathbf{C}_n^e}{\partial (\mathbf{X}_B^e)^T}. \quad (3.6)$$

The second term on the right hand side of this equation arises from the fact that the b-frame to e-frame rotation matrix given in eq. (2.2) also depends on  $\mathbf{X}_B$  via the ellipsoidal coordinates used in eq. (2.3). The partial derivatives of  $\mathbf{C}_n^e$  w.r.t.  $\mathbf{X}_B$  can best be calculated numerically when needed. However, the magnitude of the term in brackets is the length of the lever arm. The elements of the right most term correspond to the rotation of the North-, East- and Down-axes as one moves along the ellipsoid. These elements do not exceed about  $1/(6.3 \times 10^6)$  rad/m. The combined effect of the whole term is negligible if it is less than 0.5 mm (i.e. half the standard deviation of high-precision carrier phase measurements). We easily find that this is the case if the product of lever arm and error of the approximate/predicted position is bounded by:

$$\|\mathbf{X}_i^b\| \cdot \|d\mathbf{X}_B^e\| \leq 3 \cdot 10^3 \text{ m}^2. \quad (3.7)$$

This is certainly the case for the scenarios described in section 1. So we have with sufficient accuracy:

$$\frac{\partial \mathbf{X}_i^e}{\partial (\mathbf{X}_B^e)^T} = \mathbf{I} \quad (3.8)$$

and

$$\frac{\partial \phi_i^j}{\partial (\mathbf{X}_B^e)^T} = -(\mathbf{a}_{ij}^e)^T. \quad (3.9)$$

The measurement also includes information on the attitude of the platform if the antenna phase

center does not coincide with the platform origin, i.e. if  $\mathbf{X}_i^b \neq \mathbf{0}$ . This attitude must necessarily be estimated along with the platform position. So, we also need the derivatives of the carrier phase measurements w.r.t. the attitude parameters. It is possible to estimate corrections of the assumed approximate yaw, pitch and roll values directly. However, it is easier to follow an approach well known from inertial navigation, see e.g. [5, §5.3], and introduce an additional rotation matrix such that

$$\mathbf{C}_b^e := \delta \mathbf{C}_\psi \cdot (\mathbf{C}_b^e)_o \quad (3.10)$$

with

$$\delta \mathbf{C}_\psi := \mathbf{R}_3(\psi_3) \mathbf{R}_2(\psi_2) \mathbf{R}_1(\psi_1), \quad (3.11)$$

$$(\mathbf{C}_b^e)_o := \mathbf{C}_n^e \cdot \mathbf{C}_b^n(\alpha_o, \chi_o, \eta_o). \quad (3.12)$$

The sequential rotations about the first, second and third axis on the right hand side of eq. (3.11) are modeled using rotation matrices of the same type as explained in section 2. Eq. (3.12) defines an approximation of the entire b-frame to e-frame rotation matrix computed from fixed values of yaw, pitch and roll (e.g. the predicted values), and from the actual position of the b-frame origin. We assume that this approximation differs from the true rotation by less than 2 deg. This is achievable in practical applications either by iterated adjustment or by suitable prediction using a Kalman Filter. So, the second matrix on the right hand side of (3.12) will be treated as a fixed term subsequently, while the entire b-frame to e-frame rotation (3.10) depends on the unknown location and the unknown additional rotations  $\psi_1, \psi_2, \psi_3$ .

Once the values of these angles and of the platform coordinates have been estimated, the corresponding b-frame to e-frame rotation matrix

$$\hat{\mathbf{C}}_b^e := \mathbf{R}_3(\hat{\psi}_3) \cdot \mathbf{R}_2(\hat{\psi}_2) \cdot \mathbf{R}_1(\hat{\psi}_1) \cdot \mathbf{C}_n^e(\hat{\mathbf{X}}_B^e) \cdot \mathbf{C}_b^n(\alpha_o, \chi_o, \eta_o) \quad (3.13)$$

can be computed. After left-multiplication of this matrix by  $[\mathbf{C}_n^e(\hat{\mathbf{X}}_B^e)]^T$  the yaw, pitch and roll angles  $\hat{\alpha}, \hat{\chi}, \hat{\eta}$  can be extracted from the resulting matrix using the parameterization as of eq. (2.4). This shows that it is actually not necessary to estimate these angles directly. The advantage of the proposed approach is a considerable simplification of the required terms if the  $\psi_i$  are small, i.e. if the prediction of yaw, pitch and roll is accurate, as will be shown next.

For small  $\psi_k$  we may write

$$\delta \mathbf{C}_\psi \approx \mathbf{I} - \Psi, \quad \Psi = \begin{bmatrix} 0 & -\psi_3 & \psi_2 \\ \psi_3 & 0 & -\psi_1 \\ -\psi_2 & \psi_1 & 0 \end{bmatrix} \quad (3.15)$$

and thus

$$\mathbf{C}_b^e \approx (\mathbf{I} - \Psi) \cdot (\mathbf{C}_b^e)_o. \quad (3.16)$$

The error of this approximation is on the order of  $\psi^2$  (e.g.,  $10^{-3}$  if the predicted attitude has an error of about 2 deg). This is not negligible for calculating the carrier-phase measurement or for carrying out actual transformations using eq. (2.1); so these steps need to be carried out using eq. (3.11). However, eq. (3.16) is sufficiently accurate for estimating the attitude errors. For this purpose, the angles  $\psi_k$  are collected in a  $3 \times 1$  vector  $\boldsymbol{\psi}$ , and the related partial derivatives needed for parameter estimation in a linearized model are obtained from (2.1) with (3.16) as:

$$\frac{\partial \mathbf{X}_i^e}{\partial \boldsymbol{\psi}^T} = \begin{bmatrix} 0 & -Z_o & Y_o \\ Z_o & 0 & -X_o \\ -Y_o & X_o & 0 \end{bmatrix} \text{ with } \begin{bmatrix} X_o \\ Y_o \\ Z_o \end{bmatrix} := (\mathbf{C}_b^e)_o \cdot \mathbf{X}_i^b \quad (3.17)$$

Using (3.17), (3.4) and the definition of the vector cross product  $\times$  one can easily verify that

$$\frac{\partial \phi_i^j}{\partial \boldsymbol{\psi}^T} = \frac{\partial \phi_i^j}{\partial (\mathbf{X}_i^e)^T} \cdot \frac{\partial \mathbf{X}_i^e}{\partial \boldsymbol{\psi}^T} = -(\mathbf{a}_{ij}^e \times [(\mathbf{C}_b^e)_o \cdot \mathbf{X}_i^b])^T \quad (3.18)$$

The error of these partial derivatives is on the order of  $\psi^2 \cdot \|\mathbf{X}_i^b\|$  and is negligible for parameter estimation if

$$\psi^2 \cdot \|\mathbf{X}_i^b\| \cdot |\boldsymbol{\psi}| = |\boldsymbol{\psi}^3| \cdot \|\mathbf{X}_i^b\| \leq 5 \times 10^{-4} \text{ m} \quad (3.19)$$

i.e., if the error of the predicted attitude is less than about 2 deg.

The linearized observation equations of the pseudorange measurements  $P_i^j$  do not differ from those of the carrier-phase measurements as far as the relation to platform position and attitude is concerned. Thus eqs. (3.9) and (3.18) also hold for the pseudorange measurements if  $\phi$  is replaced by  $P$ . Using these partial derivatives for computing the elements of the measurement matrix (and the usual ones with respect to other parameters like clock errors, atmospheric corrections or ambiguities, as needed), the platform position and orientation can be estimated from pseudorange or carrier-phase observations, e.g. using the Least-Squares method within a Gauß-Markov-Model (GMM) for the static case

or a Kalman Filter for kinematic processing. Of course, the linearized equations using the above partial derivatives can easily be transformed into those of the DD observations by pre-multiplication with a DD-operator matrix. For illustration, we will show a numeric example in section 5.

#### 4. Velocity and attitude rate

The one-way Doppler measurement between the receiving antenna  $i$  and the satellite  $j$ , can be expressed in units of m/s as

$$D_i^j = [\dot{\mathbf{X}}_i^e - \dot{\mathbf{X}}_j^e]^T \mathbf{a}_{ij}^e \cdot (1 - \delta t_i) \pm \dots \quad (4.1)$$

with

$\dot{\mathbf{X}}_i^e$  ...receiver velocity expressed in e-frame (in m/s)

$\dot{\mathbf{X}}_j^e$  ...satellite velocity expressed in e-frame with Sagnac correction applied (in m/s)

$\delta t_i$  ...receiver clock drift (in s/s)

Again, the focus is on those terms of the observation equation which require different treatment than in the single-antenna case. So, all other terms have been omitted in eq. (4.1). A comprehensive derivation of the entire Doppler observation equation suitable for obtaining estimated receiver velocity at the mm/s level is given in [12].

The linearized observation equation is computed using the following sufficiently accurate derivatives, see e.g. [12, p. 73]:

$$\frac{\partial D_i^j}{\partial (\dot{\mathbf{X}}_i^e)^T} = (\mathbf{a}_{ij}^e)^T (1 - \delta t_i) \quad (4.2)$$

$$\frac{\partial D_i^j}{\partial (\mathbf{X}_i^e)^T} = \frac{(\dot{\mathbf{X}}_j^e - \dot{\mathbf{X}}_i^e)^T}{\|\dot{\mathbf{X}}_j^e - \dot{\mathbf{X}}_i^e\|} \cdot (\mathbf{I} - \mathbf{a}_{ij}^e \cdot (\mathbf{a}_{ij}^e)^T) \quad (4.3)$$

However, in the present context we do not estimate the velocity of the individual antenna but rather that of the platform. So we need to apply again the chain rule i.e.,

$$\frac{\partial D_i^j}{\partial \mathbf{p}^T} = \frac{\partial D_i^j}{\partial (\dot{\mathbf{X}}_i^e)^T} \cdot \frac{\partial \dot{\mathbf{X}}_i^e}{\partial \mathbf{p}^T} + \frac{\partial D_i^j}{\partial (\mathbf{X}_i^e)^T} \cdot \frac{\partial \mathbf{X}_i^e}{\partial \mathbf{p}^T} \quad (4.4)$$

to calculate the derivation of eq. (4.1) with respect to the velocity and position of the platform, the attitude and the attitude rate (any one of those

represented by  $\mathbf{p}$  in eq. 4.4). The last partial derivative on the right hand side has already been computed above for  $\mathbf{p} = \mathbf{X}_B^e$  (eq. 3.8) and  $\mathbf{p} = \boldsymbol{\psi}$  (eq. 3.17); it is  $\mathbf{0}$  for the other two vectors  $\mathbf{p} = \mathbf{X}_B^e$  and  $\mathbf{p} = \boldsymbol{\psi}$ .

From (2.1) and (3.10) we obtain by differentiating w.r.t. time and taking into account that the antenna is fixed on the platform:

$$\dot{\mathbf{X}}_i^e = \dot{\mathbf{X}}_B^e + \delta\dot{\mathbf{C}}_\psi \cdot (\mathbf{C}_b^e)_o \cdot \mathbf{X}_i^b + \delta\mathbf{C}_\psi \cdot \dot{\mathbf{C}}_n^e \cdot \mathbf{C}_b^e(\alpha_o, \chi_o, \eta_o) \cdot \mathbf{X}_i^b \quad (4.5)$$

The term including  $\dot{\mathbf{C}}_n^e$  affects the Doppler observation by less than

$$\left\| \dot{\mathbf{X}}_B^e \cdot \left\| \mathbf{X}_i^b \right\| / R \leq 1.6 \cdot 10^{-5} \text{ m/s} \quad (4.6)$$

where  $R$  is the radius of curvature of the earth, and the maximum dimension and speed of the platform as defined in sec. 1 have been used for computing the numeric value. This term is negligible for all practical purposes considered herein. So, we have with sufficient accuracy

$$\dot{\mathbf{X}}_i^e = \dot{\mathbf{X}}_B^e + \delta\dot{\mathbf{C}}_\psi \cdot (\mathbf{C}_b^e)_o \cdot \mathbf{X}_i^b \quad (4.7)$$

and consequently

$$\frac{\partial \dot{\mathbf{X}}_i^e}{\partial (\dot{\mathbf{X}}_B^e)^T} = \mathbf{I} \quad (4.8)$$

The Doppler observation depends on  $\mathbf{X}_B^e$  via  $\mathbf{C}_n^e$  which is part of  $(\mathbf{C}_b^e)_o$ . However, the effect on the linearized observation equation is negligible (less than 0.5 mm/s) if

$$\left| \dot{\boldsymbol{\psi}} \cdot \left\| \mathbf{X}_i^b \right\| \cdot \left\| d\mathbf{X}_B^e \right\| \leq 3 \cdot 10^3 \text{ m}^2/\text{s} \quad (4.9)$$

which is clearly the case for the scenarios considered herein, since a prediction of the platform position with sufficiently low error  $d\mathbf{X}_B^e$  (less than 500 m) can easily be found. So, we have with sufficient accuracy:

$$\frac{\partial \dot{\mathbf{X}}_i^e}{\partial \mathbf{X}_B^e} = \mathbf{0} \quad (4.10)$$

The term including the time derivative of  $\delta\mathbf{C}_\psi$  in eq. (4.7) is neither negligible for computing the reduced observation nor for computing the partial derivatives. These can be written conveniently as

$$\frac{\partial \dot{\mathbf{X}}_i^e}{\partial \boldsymbol{\psi}^T} = \left( \mathbf{I}_3 \otimes [(\mathbf{C}_b^e)_o \cdot \mathbf{X}_i^b]^T \right) \cdot \frac{\partial \text{vec}(\delta\dot{\mathbf{C}}_\psi)}{\partial \boldsymbol{\psi}^T} \quad (4.11)$$

where  $\delta\dot{\mathbf{C}}_\psi$  and its derivation w.r.t.  $\boldsymbol{\psi}$  needs to be computed from the correct equation (3.11) rather than from (3.15), i.e. from

$$\begin{aligned} \delta\dot{\mathbf{C}}_\psi = & \mathbf{R}_3(\psi_3)\mathbf{R}_2(\psi_2) \begin{bmatrix} 0 & 0 & 0 \\ 0 & -\sin\psi_1 & \cos\psi_1 \\ 0 & -\cos\psi_1 & -\sin\psi_1 \end{bmatrix} \cdot \dot{\boldsymbol{\psi}}_1 + \\ & + \mathbf{R}_3(\psi_3) \begin{bmatrix} -\sin\psi_2 & 0 & -\cos\psi_2 \\ 0 & 0 & 0 \\ \cos\psi_2 & 0 & -\sin\psi_2 \end{bmatrix} \mathbf{R}_1(\psi_1) \cdot \dot{\boldsymbol{\psi}}_2 + \\ & + \begin{bmatrix} -\sin\psi_3 & \cos\psi_3 & 0 \\ -\cos\psi_3 & -\sin\psi_3 & 0 \\ 0 & 0 & 0 \end{bmatrix} \mathbf{R}_2(\psi_2)\mathbf{R}_1(\psi_1) \cdot \dot{\boldsymbol{\psi}}_3 \end{aligned} \quad (4.12)$$

Since the dependence of the velocity vector of the antenna on the attitude rate is also via  $\delta\dot{\mathbf{C}}_\psi$  we obtain in complete analogy

$$\frac{\partial \dot{\mathbf{X}}_i^e}{\partial \boldsymbol{\psi}^T} = \left( \mathbf{I}_3 \otimes [(\mathbf{C}_b^e)_o \cdot \mathbf{X}_i^b]^T \right) \cdot \frac{\partial \text{vec}(\delta\dot{\mathbf{C}}_\psi)}{\partial \boldsymbol{\psi}^T} \quad (4.13)$$

Also this expression needs to be evaluated using the strict equation (4.11) rather than one obtained from the approximation (3.15). However, the columns of the  $9 \times 3$  matrix  $\partial \text{vec}(\delta\dot{\mathbf{C}}_\psi) / \partial \boldsymbol{\psi}^T$  are simply obtained from the matrices preceding  $\dot{\boldsymbol{\psi}}_1, \dot{\boldsymbol{\psi}}_2, \dot{\boldsymbol{\psi}}_3$  in eq. (4.12) by vectorizing.

Finally, we get the required partial derivatives of the Doppler observations with respect to the unknown parameters of the platform by inserting the respective intermediate results into (4.4). This yields:

$$\frac{\partial D_i^j}{\partial (\mathbf{X}_B^e)^T} = \frac{(\dot{\mathbf{X}}_j^e - \dot{\mathbf{X}}_i^e)^T}{\left\| \mathbf{X}_j^e - \mathbf{X}_i^e \right\|} \cdot \left( \mathbf{I} - \mathbf{a}_{ij}^e \cdot (\mathbf{a}_{ij}^e)^T \right) \quad (4.14)$$

$$\frac{\partial D_i^j}{\partial (\dot{\mathbf{X}}_B^e)^T} = (\mathbf{a}_{ij}^e)^T (1 - \delta i_i) \quad (4.15)$$

$$\begin{aligned} \frac{\partial D_i^j}{\partial \boldsymbol{\psi}^T} = & (\mathbf{a}_{ij}^e)^T \left( \mathbf{I}_3 \otimes [(\mathbf{C}_b^e)_o \cdot \mathbf{X}_i^b]^T \right) \cdot \\ & \cdot \frac{\partial \text{vec}(\delta\dot{\mathbf{C}}_\psi)}{\partial \boldsymbol{\psi}^T} (1 - \delta i_i) \end{aligned} \quad (4.16)$$

$$\begin{aligned} \frac{\partial D_i^j}{\partial \boldsymbol{\psi}^T} = & (\mathbf{a}_{ij}^e)^T \left( \mathbf{I}_3 \otimes [(\mathbf{C}_b^e)_o \cdot \mathbf{X}_i^b]^T \right) \cdot \\ & \cdot \frac{\partial \text{vec}(\delta\dot{\mathbf{C}}_\psi)}{\partial \boldsymbol{\psi}^T} (1 - \delta i_i) \end{aligned} \quad (4.17)$$

When deriving (4.16) the contribution by the product of (4.3) and (3.17) has been neglected because it is too small. Further simplifications are

possible if it can be assured that the predicted coordinates are accurate to within a few meters – (4.14) is negligible then –, if the receiver exhibits a low oscillator frequency offset (unlike some low-cost receivers) – in this case,  $\delta\dot{t}_i$  is negligible in the above equations –, and if the predicted values of  $\psi$  are exactly 0 (i.e., if yaw, pitch and roll as used in eq. (3.12) are updated in case the estimated or predicted value of  $\psi$  were non-zero without such an update) – (4.16) can then be expressed using

$$\frac{\partial \text{vec}(\delta\dot{\mathbf{C}}_{\psi}^b)}{\partial \dot{\psi}^T} = \begin{bmatrix} 0 & 0 & 0 & \dot{\psi}_2 & -\dot{\psi}_1 & 0 & \dot{\psi}_3 & 0 & \dot{\psi}_1 \\ -\dot{\psi}_2 & 0 & 0 & \dot{\psi}_1 & 0 & 0 & 0 & \dot{\psi}_3 & -\dot{\psi}_2 \\ -\dot{\psi}_3 & 0 & 0 & 0 & -\dot{\psi}_3 & 0 & \dot{\psi}_1 & \dot{\psi}_2 & 0 \end{bmatrix}^T \tag{4.18}$$

and (4.17) can be replaced by

$$\frac{\partial D_i^j}{\partial \dot{\psi}^T} = -\mathbf{a}_{ij}^e \times [(\mathbf{C}_b^e)_o \cdot \mathbf{X}_i^b] (1 - \delta\dot{t}_i) \tag{4.19}$$

**5. Numeric example**

For demonstration, we briefly analyze the situation shown in Fig. 6. We will predict the precision of the position, velocity and attitude of the platform as estimated on an epoch-by-epoch basis using single-frequency GPS DD carrier-phase observations and undifferenced Doppler observations. Three GPS antennas (A1, A2, A3) are mounted on a nearly horizontal platform, and a fourth GPS antenna is setup about 100 m east at a stationary reference site (REF). All antennas track satellites at elevations higher than 15 deg.

When evaluating a single epoch of data here, we assume that the carrier-phase integer ambiguities have already been resolved and that the pseudorange observations are only used for data pre-processing. So, the parameter vector contains 15 elements, namely the e-frame coordinates and velocities of B, the attitude corrections  $\psi_k$  and their rate (as nuisance parameters), and the receiver clock

drift of the three platform receivers (no Doppler observations are used at REF). The actual GPS satellite distribution on Feb 1, 2011, 1:30 UTC as seen in Vienna, Austria has been arbitrarily chosen for demonstration purposes. Two scenarios are distinguished: (a) the antennas are not affected by any signal obstruction (obstacle in Fig. 6 is lower than the antennas), (b) the obstacle is 2 m higher than the antennas and thus causes significant but different obstruction to each platform antenna.

The observation matrices of the undifferenced carrier-phase and Doppler observations of a single epoch are set up using the partial derivatives derived in sec. 3 and 4. The undifferenced observations are assumed to be uncorrelated, to have standard deviations proportional to  $1/\sin E$ , and to have a standard deviation of 2 mm and 2 mm/s, respectively, in zenith direction. Double differencing of the carrier-phase observations and the associated variance propagation are taken into account properly by multiplication of the original observations and observation matrix with a DD operator matrix before estimating the unknown parameters using weighted least squares adjustment.

The satellite visibility for scenario (b) and about half an hour of data is shown in Fig. 7. The epoch actually processed lies within this period. The grey shading indicates obstructed portions of the sky. Obstructed satellites are shown in grey color; their data are not used when evaluating scenario (b). It is clear from this figure that the position of antenna A3 could not be estimated individually (less than 4 satellites available), and that the geometry for estimating the positions of the other two platform antennas is rather poor. This is also confirmed by the DOP values reported in Tab. 1. These values represent the RDOP, see [3], i.e. the trace of the cofactor matrix of the coordinates estimated in relative mode. Using all available data to estimate the origin of the platform rather than the individual antenna, we obtain a DOP of 6.4, which is not excellent, but better than any of the individual site’s DOP. Furthermore, only the combination of the data allows obtaining an estimate of the platform position at all, in this case.

If the obstacle on the platform does not cause any GPS signal obstruction, the satellite visibility at each of the platform antennas is identical to the one at the reference station (Fig. 7, top left). In this case, the RDOP is 5.8 when determining each one of the platform antennas individually with REF as reference station, see Tab. 1. This

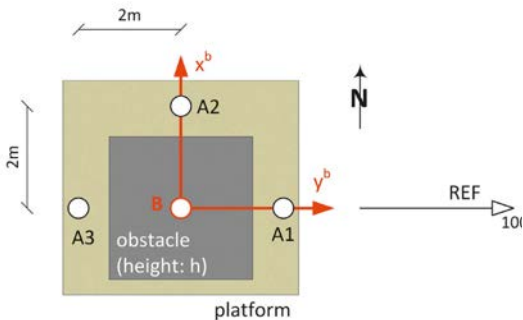


Fig. 6: Setup used for numeric example

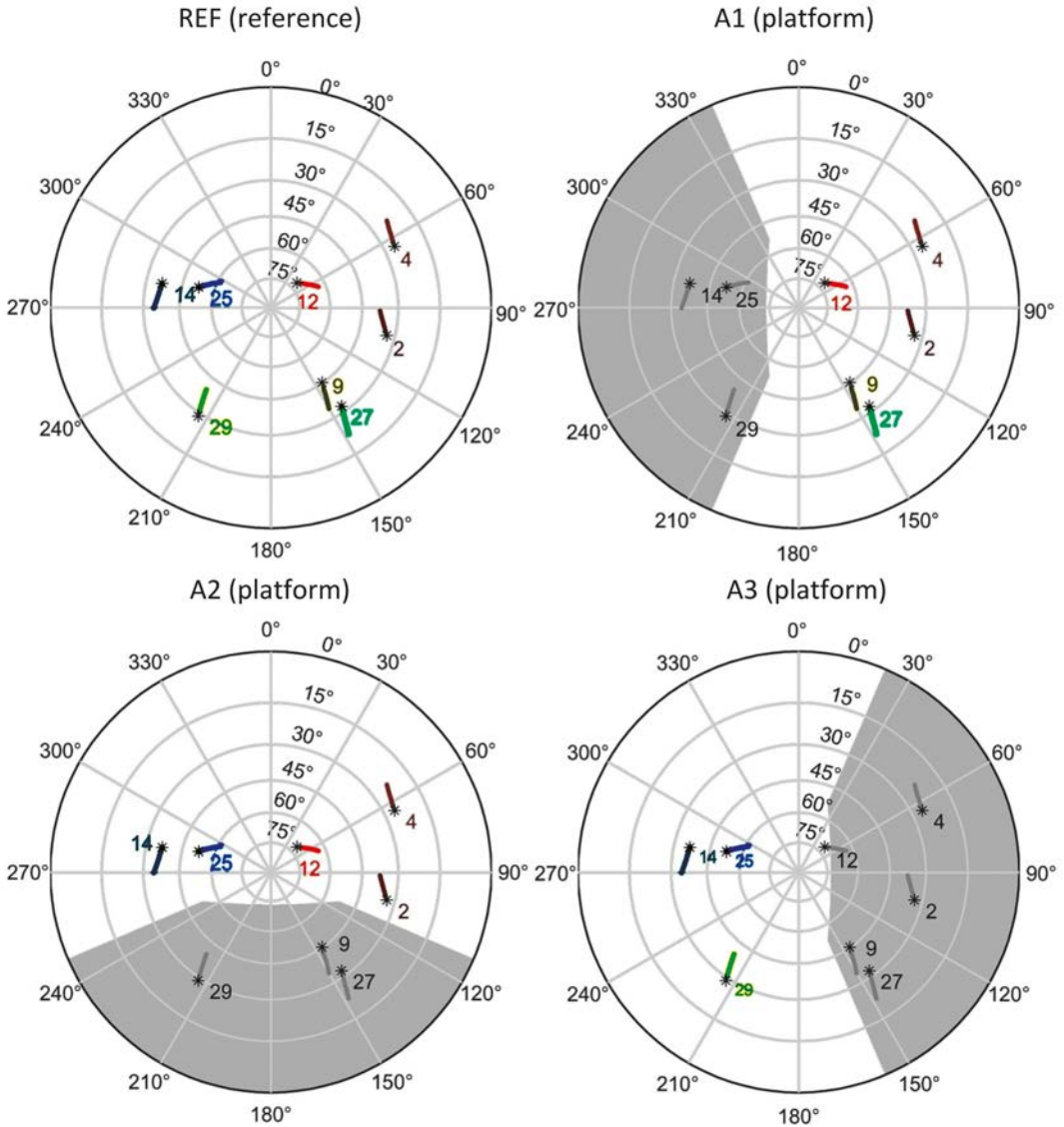


Fig. 7: Satellite visibility at the reference station and at the three antenna sites on the platform as used for the numeric example, scenario (b) i.e., with obstruction

indicates that the satellite distribution is not ideal even without obstruction (however, it is a real situation). The DOP value reduces to 4.9 if all data are combined to estimate the position of the platform origin directly which indicates significantly better precision.

The predicted standard deviation of all estimated parameters except the clock drift is given in Tab. 2 for both scenarios. The values refer to the direct estimation of the 15 states mentioned above and give an impression of

the attainable precision, even in a suboptimum case like the one chosen. While the standard deviations of the estimated coordinates and velocities are virtually independent of platform size (and the results of the numeric examples are thus also valid for the robot shown in Fig. 1), the standard deviations of the attitude and attitude rates scale linearly with antenna separation (if the obstruction masks remain unaltered).

Of course, the measures of precision do not reflect the reliability, in particular the magnitude

Point ID	No obstacle	With obstacle
A1	5.8	13.4
A2	5.8	8.4
A3	5.8	$\infty$
B (platform origin)	4.9	6.4

Tab. 1: DOP values indicating relative precision of 3D-coordinates (based on elevation dependent variances of the one-way observations)

of potentially undetected gross errors (minimum detectable biases) and their effect on the estimates (external reliability). An analysis of these values shows that errors between 10 and 20 mm (e.g., typical multipath effects) would go unnoticed with most of the observations, and even larger errors with some of them, in particular in the scenario with obstruction. The corresponding effect on the coordinates reaches about 15 mm in the case without obstruction but exceeds 50mm in the other case.

This shows that multipath suppression e.g. by microwave absorbing screens as proposed in sec. 1 may be very useful in case reflections at parts of the platform are likely. Only such means would allow practically achieving accuracies like the standard deviations given in Tab. 2. Furthermore, in reality one would try to apply 4 rather than 3 antennas, and carry out parameter estimation using a Kalman Filter if the platform is kinematic, or static processing in a Gauß-Markov model if the platform is static within measurement precision. This increases the redundancy, reduces the standard deviation of the results, increases the probability of correctly detecting and identifying outliers, and reduces the impact of potentially missed outliers. The equations derived above are applicable to both processing schemes and to all GNSS, not only to GPS.

**6. Conclusion and outlook**

We have presented observation equations of GNSS carrier-phase and Doppler observations for direct estimation of platform position, velocity and attitude. The derived terms refer to the

undifferenced observations and can thus easily be used for any linear combinations of observations, including single- and double-differences of equal types of observations.

Often, objects on a platform simultaneously cause signal obstruction and multipath effects thus deteriorating both precision and accuracy of the results obtained using GNSS antennas on the platform. However, the combined processing of data from multiple antennas – and potentially the shading of multipath signals using microwave absorbing material – may allow mitigating this problem. This was demonstrated above using a numeric example where the platform state can be estimated precisely from the data of three platform antennas using the proposed algorithm.

The derived equations can be used without any modification for processing GPS pseudorange observations and corresponding observations obtained from other/future GNSS. Currently, the algorithms are being extended by dynamic models of the platform and are being implemented in a Kalman Filter software for subsequent experimental validation using the mobile robot shown in Fig. 1. These experiments will also include the use of microwave absorbing foam for multipath mitigation. Further investigations also comprise proper handling of time lags between non-synchronized receivers. Such lags have not been considered above, because the data output epochs of typical geodetic GPS receivers are synchronized to GPS time at the micro-second level or better and the lags are therefore negligible with respect to the applications and assumptions discussed above. However, the use of low-cost equipment might be attractive for certain applications, but such receivers may synchronize only loosely with a common time basis and consequently, the lags of the individual receivers on the platform need to be taken into account.

	Position [mm]			Attitude [0.1 deg]			Velocity [mm/s]			Rotation rate [0.01 deg/s]		
	<i>N</i>	<i>E</i>	<i>U</i>	$\eta$	$\chi$	$\alpha$	<i>N</i>	<i>E</i>	<i>U</i>	$\dot{\psi}_1$	$\dot{\psi}_2$	$\dot{\psi}_3$
No obstacle	3.8	2.3	8.7	1.3	2.1	0.5	2.0	1.3	5.1	0.2	0.4	0.2
With obstacle	4.7	4.8	11.0	2.5	3.2	1.0	3.4	3.3	8.5	0.3	0.6	0.3

Tab. 2: Standard deviation ( $1\sigma$ ) of estimated parameters for the two scenarios discussed in the text (*N*: North, *E*: East, *U*: Up)

## References

- [1] *Boccia L, Pace P, Amendola G, Di Massa G (2008)*: Low multipath antennas for GNSS-based attitude determination systems applied to high-altitude platforms
- [2] *Cohen CE (1992)*: Attitude Determination Using GPS. PhD Dissertation, Stanford University, California, USA, 184p
- [3] *Goat C (1988)*: Investigation of an alternate method of processing global positioning survey data collected in kinematic mode. In: Groten E, Strauß R (Eds) GPS-Techniques Applied to Geodesy and Surveying. Lecture Notes in Earth Sciences 19, Springer, Berlin, pp93-106
- [4] *Georgiadou Y, Kleusberg A (1988)*: On carrier signal multipath effects in relative GPS positioning. *Manuscripta Geodaetica* 13, pp 172-179
- [5] *Jekeli C (2001)*: Inertial Navigation Systems with Geodetic Applications. Walter de Gruyter, Berlin – New York, 352p
- [6] *Kleusberg A (1995)*: Mathematics of Attitude Determination with GPS. *GPS World*, Innovation Column, September, pp 72-78
- [7] *Leick A (2004)*: GPS Satellite Surveying. John Wiley & Sons, Hoboken, 435p
- [8] *Saalfeld A (1999)*: Generating basis sets of double-differences. *Journal of Geodesy* 73, pp 291-297
- [9] *Teunissen P, Kleusberg A (1998)*: GPS for Geodesy. 2<sup>nd</sup>ed, Springer Verlag, Berlin - Heidelberg - New York, 650p
- [10] *Ueno M, Santerre R, Babineau S (1997)*: Impact of antenna configuration on GPS attitude determination. In: Proc 9th World Congress International Association of Institutes of Navigation (IAIN), Amsterdam, The Netherlands, 18-21 November, 8p
- [11] *Ueno M, Santerre R, Kleusberg A (1999)*: Direct determination of angular velocity using GPS. *Journal of the Royal Institute of Navigation* 53(2), pp 371-379
- [12] *Wieser A (2007)*: GPS based velocity estimation and its application to an odometer. *Engineering Geodesy - TU Graz*, Shaker Verlag, Aachen, ISBN 978-3-8322-6460-4

## Contacts

Univ. Prof. DI Dr. **Andreas Wieser**, Vienna University of Technology, Institute of Geodesy and Geophysics, Gußhausstraße 27-29/1283, 1040 Vienna, Austria.  
E-Mail: andreas.wieser@tuwien.ac.at

**Roland Aschauer**, BSc, Unionstraße 47/9, 4020 Linz.  
E-Mail: e0526796@student.tuwien.ac.at 